Atmos. Chem. Phys. Discuss., doi:10.5194/acp-2016-662, 2016
Manuscript under review for journal Atmos. Chem. Phys.
Published: 22 August 2016
© Author(s) 2016. CC-BY 3.0 License.

Atmospheric Chemistry and Physics Discussions

# Molecular distributions and stable carbon isotope compositions of oxalic acid and related SOA in Beijing before, during and after the 2014 APEC

Jiayuan Wang[1,3], Gehui Wang[1,2,3,4,*], Jian Gao[5,6,*], Han Wang[5,6], Yanqin Ren[1,3], Jianjun Li[1], Bianhong Zhou[1], Can Wu[1,3], Lu Zhang[1,3], Shulan Wang[5,6], Fahe Chai[5,6]

[1]Key Lab of Aerosol Chemistry and Physics, State Key Laboratory of Loess and Quaternary Geology, Institute of Earth Environment, Chinese Academy of Sciences, Xi'an 710061, China
[2]School of Human Settlements and Civil Engineering, Xi'an Jiaotong University, Xi'an 710079, China
[3]University of Chinese Academy of Sciences, Beijing, China
[4]Center for Excellence in Urban Atmospheric Environment, Institute of Urban Environment, Chinese Academy of Sciences, Xiamen, China
[5]State Key Laboratory of Environmental Criteria and Risk Assessment, Chinese Research Academy of Environmental Sciences, Beijing 10084, China
[6]Collaborative Innovation Center of Atmospheric Environment and Equipment Technology, Nanjing 210000, China

*Correspondence to*: Gehui Wang (wanggh@ieecas.cn) and Jian Gao (gaojian@craes.org.cn)

Atmos. Chem. Phys. Discuss., doi:10.5194/acp-2016-662, 2016
Manuscript under review for journal Atmos. Chem. Phys.
Published: 22 August 2016
© Author(s) 2016. CC-BY 3.0 License.

Atmospheric Chemistry and Physics Discussions

**Abstract**: To ensure the good air quality for the 2014 APEC, stringent emission controls were implemented in Beijing and its surrounding regions, leading to a significant reduction in $PM_{2.5}$ loadings. To investigate the impacts of the emission controls on aerosol composition and formation, high-volume $PM_{2.5}$ samples were collected in Beijing from 08/10/2014 to 24/11/2014 and determined for secondary inorganic ions (SIA, i.e., $SO_4^{2-}$, $NO_3^-$ and $NH_4^+$), dicarboxylic acids, keto-carboxylic acid and α-dicarbonyls, as well as stable carbon isotope composition of oxalic acid ($C_2$). Our results showed that SIA in $PM_{2.5}$ are 52 ± 47, 18 ± 13 and 33 ± 29 μg $m^{-3}$ before-, during- and after-APEC, accounting for 29%, 18% and 20% of $PM_{2.5}$, respectively. As the leading dicarboxylic acid, $C_2$ in $PM_{2.5}$ during the three phases are 502 ± 564, 101 ± 69 and 166 ± 157 ng $m^{-3}$, accounting for 46%, 31% and 34% of total detected organic compounds (TDOC, i.e., the sum of dicarboxylic acids, keto-carboxylic acids and α-dicarbonyls). The higher values of concentrations and relative abundances of SIA and $C_2$ before-APEC suggest that $PM_{2.5}$ aerosols during this period are more enriched with secondary products, mainly due to an enhanced photochemical oxidation under the higher temperature and more humid conditions. SIA, $C_2$ and related SOA in $PM_{2.5}$ during-APEC were 2−4 times lower than those before-APEC.

$C_2$ in the regional air masses, which mostly occurred before-APEC, are abundant and enriched in $^{13}C$. On the contrary, $C_2$ in the long-range transport air masses, which mostly occurred during-APEC, is much less abundant but still enriched in $^{13}C$. In the local air masses, which mostly occurred after-APEC, $C_2$ concentration is lower than that before-APEC but higher than that during-APEC and enriched in lighter $^{12}C$. A comparison on chemical composition of $PM_{2.5}$ and $\delta^{13}C$ values of $C_2$ in two events that are characterized by the highest $PM_{2.5}$ levels before- and after-APEC, respectively, further showed that after-APEC SIA and TDOC are much

Atmos. Chem. Phys. Discuss., doi:10.5194/acp-2016-662, 2016
Manuscript under review for journal Atmos. Chem. Phys.
Published: 22 August 2016
© Author(s) 2016. CC-BY 3.0 License.

Atmospheric Chemistry and Physics Discussions

less abundant and fine aerosols are enriched with primary organics and relatively fresh, compared with those before-APEC. Such reduction in secondary aerosols after-APEC, along with a similar reduction during-APEC, is largely due to the decreasing temperatures. Our results indicate that the significant reduction in $PM_{2.5}$ during-APEC is mainly due to the efficient emission controls, but the effect of the decreasing temperatures, which suppressed secondary aerosol production, may also take an important role.

**Key words**: Secondary organic aerosols; Emission controls; Sources and formation mechanisms; Aqueous-phase oxidation; Aerosol acidity and water content.

Atmos. Chem. Phys. Discuss., doi:10.5194/acp-2016-662, 2016
Manuscript under review for journal Atmos. Chem. Phys.
Published: 22 August 2016
© Author(s) 2016. CC-BY 3.0 License.

Atmospheric Chemistry and Physics Discussions

## 1. Introduction

Atmospheric aerosols profoundly impact the global climate directly by scattering and absorbing solar radiation and indirectly by affecting cloud formation and distribution via acting as cloud condensation nuclei (CCN) and ice nuclei (IN). Moreover, atmospheric aerosols exert negative effects on human health because of their toxicity. Due to fast urbanization and industrialization, high level of atmospheric fine particle ($PM_{2.5}$) pollution has been a persistent problem in many cities of China since the nineties of last century (van Donkelaar et al., 2010). As the capital of China and one of the largest megacities in the world, Beijing has suffered from frequent severe haze pollution especially in winter, affecting more than 21 million people by the end of 2014 (Beijing Municipal Bureau of Statistics, 2015) and causing billions of economic loses (Mu and Zhang, 2013). To improve the air quality Beijing government has put many efforts to reduce the pollutant emissions (i.e., $SO_2$, NOx, dust, and volatile organic compounds (VOCs)) from a variety of sources.

The 2014 Asia-Pacific Economic Cooperation (APEC) summit was hosted in Beijing from the $5^{th}$ to $11^{th}$ November. To ensure good air quality for the summit, a joint strict emission control program was conducted from $3^{rd}$ November 2014 in Beijing and its neighboring provinces including Inner Mongolia, Shanxi, Hebei and Shandong provinces. During this period thousands of factories and power plants with high emissions were shut down and/or halted, all the construction activities were stopped and the numbers of on-road vehicles were reduced. These strict emission controls resulted in the air quality of Beijing during the APEC period being significantly improved, leading to a decrease in $PM_{2.5}$ concentration by 59.2% and an increase in visibility by 70.2% in Beijing during the summit compared with those before the APEC (Tang et

Atmos. Chem. Phys. Discuss., doi:10.5194/acp-2016-662, 2016
Manuscript under review for journal Atmos. Chem. Phys.
Published: 22 August 2016
© Author(s) 2016. CC-BY 3.0 License.

Atmospheric Chemistry and Physics Discussions

al., 2015) and a term of "APEC-Blue" being created to refer to the good air quality. Such strong artificial intervening not only reduced $PM_{2.5}$ and its precursors' loadings in Beijing and its surrounding areas but also affected the composition and formation mechanisms of the fine particles (Sun et al., 2016).

A number of field measurements have showed that particle compositions in Beijing during wintertime haze periods are dominated by secondary aerosols (Guo et a., 2014; Huang et al, 2014; Xu et al., 2015). Rapid accumulation of particle mass in Beijing during haze formation process is often accompanied by continuous particle size growth (Guo et al, 2014; Zhang et al., 2015), which is in part due to the coating of secondary organic aerosols (SOA) on pre-existing particles (Li et al., 2010). Several studies have found that SOA production during the 2014 Beijing APEC periods significantly reduced and ascribed this reduction to the efficient regional emission control (Sun et al., 2016; Xu et al, 2015). However, up to now information of the SOA decrease on a molecular level has not been reported. Dicarboxylic acids are the major class of SOA species in the atmosphere and ubiquitously found from the ground surface to the free troposphere (Fu et al., 2008; Myriokefalitakis et al., 2011; Sorooshian et al., 2007; Sullivan et al., 2007). In the current work we measured molecular distributions of dicarboxylic acids, keto-carboxylic acids and α-dicarbonyls and stable carbon isotope composition of oxalic acid in $PM_{2.5}$ aerosols collected in Beijing before, during and after the APEC event in order to explore the impact of the APEC emission control on SOA in Beijing. We first investigated the changes in concentration and composition of dicarboxylic acids and related compounds during the three periods, then we recognized the difference in stable carbon isotope composition of oxalic acid in different air masses in Beijing during the APEC campaign. Finally we compared the different

Atmos. Chem. Phys. Discuss., doi:10.5194/acp-2016-662, 2016
Manuscript under review for journal Atmos. Chem. Phys.
Published: 22 August 2016
© Author(s) 2016. CC-BY 3.0 License.

chemical compositions of $PM_{2.5}$ during two heaviest pollution episodes. Our results indicated that in comparison with those before the event, the decrease in $PM_{2.5}$ levels during APEC 2014 was caused not only by the emission controls but also by a decreased SOA production due to the decreasing temperatures.

## 2. Experimental section

### 2.1 Sample collection

$PM_{2.5}$ samples were collected by using a high-volume sampler (Brand, USA) from 8$^{th}$ October to 24$^{th}$ November 2014 on the rooftop of a three-storey building located on the campus of China Research Academy of Environmental Sciences, which is situated in the north part of Beijing and close to the 5$^{th}$-ring road. All the $PM_{2.5}$ samples were collected onto pre-baked (450 $^{o}$C for 8 h) quartz fiber filters (Whatman 41, USA). The duration of each sample collection is 23 hr from 08:00 am of the previous day to 07:00 am of the next day. Field blanks were also collected before and after the campaign by mounting a pre-baked filter onto the sampler for 15 min without pumping air. After collection, all the filter samplers were individually sealed in aluminum foil bags and stored in a freezer (-18 $^{o}$C) prior to analysis. Daily values of $SO_2$, NOx and meteorological parameters were cited from the website of Beijing Environmental Protection Agency.

### 2.2 Sample analysis

#### 2.2.1 Elemental carbon (EC), organic carbon (OC), water-soluble organic (WSOC) and inorganic ions

Detailed methods for the analysis of EC, OC, WSOC and inorganic ions in aerosols were reported elsewhere (Li et al., 2011; Wang et al 2010). Briefly, EC and OC in the $PM_{2.5}$ samples

Atmos. Chem. Phys. Discuss., doi:10.5194/acp-2016-662, 2016
Manuscript under review for journal Atmos. Chem. Phys.
Published: 22 August 2016
© Author(s) 2016. CC-BY 3.0 License.

Atmospheric Chemistry and Physics Discussions

were determined by using DRI Model 2001 Carbon analyzer following the Interagency Monitoring of Protected Visual Environments (IMPROVE) thermal/optical reflectance (TOR) protocol (Chow et al., 2007). WSOC and inorganic ions in the samples were extracted with Milli-Q pure water and measured by using Shimadzu TOC-L CPH analyzer and Dionex-600 ion chromatography, respectively (Li et al. 2011; Wang et al 2010).

### 2.2.2 Dicarboxylic acids, keto-carboxylic acids and α-dicarbonyls

The method of analyzing $PM_{2.5}$ samples for dicarboxylic acids, ketocarboxylic acids and α-dicarbonyl has been reported elsewhere (Wang et al., 2012; Meng et al., 2014; Cheng et al., 2015). Briefly, one eighth of the filter was extracted with Milli-Q water, concentrated to near dryness, and reacted with 14% $BF_3$/butanol at 100 °C for 1 h to convert aldehyde group into dibutoxy acetal and carboxyl group into butyl ester. Target compounds in the derivatized samples were identified by GC/MS and quantified by GC-FID (Agilent GC7890A).

### 2.3. Stable carbon isotope composition of oxalic acid (C2)

Stable carbon isotope composition ($\delta^{13}C$) of $C_2$ was measured using the method developed by Kawamura and Watanabe (2004). Briefly, $\delta^{13}C$ values of the derivatized samples above were determined by gas chromatography-isotope ratio-mass spectrometry (GC-ir-MS) (Thermo Fisher, Delta V Advantage). The $\delta^{13}C$ value of $C_2$ was then calculated from an isotopic mass balance equation based on the measured $\delta^{13}C$ of the derivatizations and the derivatizing reagent (1-butanol) (Kawamura and Watanabe, 2004). Each sample was measured for three times to ensure the difference of the $\delta^{13}C$ values less than 0.2‰, and the isotope data reported here is the averaged value of the triplicate measurements.

## 3. Results and discussion

Atmos. Chem. Phys. Discuss., doi:10.5194/acp-2016-662, 2016
Manuscript under review for journal Atmos. Chem. Phys.
Published: 22 August 2016
© Author(s) 2016. CC-BY 3.0 License.

Atmospheric Chemistry and Physics Discussions

### 3.1 Variations in meteorological conditions, gaseous pollutants and major components of $PM_{2.5}$ during the Beijing 2014 APEC campaign

Based on the emission control implementation for the APEC, we divided the whole study period into three phases: before-APEC (08/10 to 02/11), during-APEC (03/11 to 12/11) and after-APEC (13/11 to 24/11). Temporal variations in meteorological parameters and concentrations of gaseous pollutants and major components of $PM_{2.5}$ during the three phases are shown in Fig. 1 and summarized in Table 1.

Temperature during the sampling campaign showed a continuous decreasing trend with averages of 13 ± 2.6 °C, 7.0 ± 1.7 °C and 4.3 ± 1.3 °C before-, during- and after-APEC periods, respectively, while relative humidity (RH) did not show a clear trend with mean values of 62 ± 19%, 47 ± 14% and 51 ± 16% during the three periods (Fig.1a and Table 1). $SO_2$ showed a similar level before- and during-APEC periods (8.8 ± 4.6 μg $m^{-3}$ versus 7.6 ± 3.9 μg $m^{-3}$) (Table 1), but increased dramatically to 23 ± 8.8 μg $m^{-3}$ after-APEC due to domestic coal burning for house heating (Fig. 1b). $NO_2$ concentration (45 ± 18 μg $m^{-3}$) during the APEC reduced by about 30% compared to that in the before- and after-APEC phases (71 ± 27 μg $m^{-3}$ versus 78 ± 29 μg $m^{-3}$) (Table 1), mainly because of the reduction of the on-road vehicle numbers, as well as the reduced productivities of power plant and industry. $O_3$ displayed a decreasing trend similar to that of temperature (Fig. 1c). $PM_{2.5}$ pollution episodes in Beijing showed a periodic cycle of 4−5 days, which is caused by the local weather cycles. Secondary inorganic ions (SIA, i.e., $SO_4^{2-}$, $NO_3^-$ and $NH_4^+$) are major components of $PM_{2.5}$ and present a temporal variation pattern similar to that of the fine particles (Fig. 1d). In the current work mass ratio of $NO_3^-/SO_4^{2-}$ in $PM_{2.5}$ during the whole study time is 1.8 ± 1.9 (Table 1), which is in agreement with the ratio (1.6−2.4)

Atmos. Chem. Phys. Discuss., doi:10.5194/acp-2016-662, 2016
Manuscript under review for journal Atmos. Chem. Phys.
Published: 22 August 2016
© Author(s) 2016. CC-BY 3.0 License.

Atmospheric Chemistry and Physics Discussions

for $PM_1$ observed during the same time by using aerosol mass spectrometry (AMS) (Sun et al., 2016). OC and EC of $PM_{2.5}$ linearly correlated each other ($R^2$=0.91) and varied periodically in a cycle similar to SIA (Fig. 1e). OC/EC ratio during the whole sampling period is 3.3 ± 0.6 (range: 2.2−4.7) with no significant differences among the three APEC phases (Table 1).

Figure 2 shows the differences in chemical composition of $PM_{2.5}$ before-, during- and after-APEC periods. $PM_{2.5}$ is 98 ± 46 μg $m^{-3}$ during-APEC, about 50% lower than that before- and after-APEC (178 ± 122 μg $m^{-3}$ versus 161 ± 100 μg $m^{-3}$), respectively. Organic matter (OM) is the most abundant component of the fine particles. Relative abundance of OM (OM, 1.6 times of OC) (Xing et al., 2013) to $PM_{2.5}$ increase from 24% before-APEC to 30% and 39% during- and after-APEC, although the mass concentration (19 ± 7.6 μg $m^{-3}$) of OC during-APEC is the lowest compared to those before- and after-APEC (26 ± 16 μg $m^{-3}$ versus 39 ± 23 μg $m^{-3}$). Sulfate, nitrate and ammonium before-APEC are 15 ± 13, 28 ± 26 and 9.0 ± 8.0 μg $m^{-3}$ (Table 1) and account for 8%, 16% and 5% of $PM_{2.5}$, respectively (Fig. 2). Their concentrations decrease to 5.3 ± 2.8, 10 ± 8.1 and 3.1 ± 2.6 μg $m^{-3}$ (Table 1) with the relative contributions to $PM_{2.5}$ down to 5%, 10% and 3% during-APEC, respectively. While after-APEC their concentrations increased to 11 ± 10, 15 ± 13 and 6.9 ± 6.4 μg $m^{-3}$ and accounted for 7%, 9% and 4% of $PM_{2.5}$. Such significant decreases in concentrations of OM and SIA during-APEC demonstrate the efficiency of the emission controls. OC/EC ratio is almost constant during the whole period, but WSOC/OC ratio decreased by 20% from 0.42 ± 0.13 before-APEC, 0.38 ± 0.16 during-APEC to 0.35 ± 0.17 after-APEC (Table 1). Since WSOC in fine aerosols consist mainly of secondary organic aerosols (SOA) (Laskin et al., 2015), the decreasing ratio of WSOC/OC probably indicates a reduced SOA production during the campaign.

Atmos. Chem. Phys. Discuss., doi:10.5194/acp-2016-662, 2016
Manuscript under review for journal Atmos. Chem. Phys.
Published: 22 August 2016
© Author(s) 2016. CC-BY 3.0 License.

Atmospheric Chemistry and Physics Discussions

### 3.2 Oxalic acid and related SOA during the Beijing 2014 APEC campaign

A homogeneous series of dicarboxylic acids ($C_2$−$C_{11}$), keto-carboxylic acid and α-dicarbonyls in the $PM_{2.5}$ samples were detected. As show in Table 2, total dicarboxylic acids during the whole study period is 593 ± 739 ng $m^{-3}$, which is lower than that observed during Campaign of Air Quality Research in Beijing 2006 (CAREBeijing ) (average 760 ng $m^{-3}$) and 2007 (average 1010 ng $m^{-3}$) (Ho et al, 2010, 2015) and the averaged wintertime concentration reported by a previous research for 14 Chinese cities (904 ng $m^{-3}$) (Ho et al, 2007). Total keto-carboxylic acid is 66 ± 81 ng $m^{-3}$, while total dicarbonyls is 126 ± 115 ng $m^{-3}$ (Table 2). These values are higher than those during CAREBeijing 2006 and 2007 (Ho et al, 2010, 2015), but close to the value observed for the 14 Chinese megacities (Ho et al, 2007). Being similar to those previous observations, oxalic acid ($C_2$) is the most abundant diacid in the 2014 APEC samples with an average of 334 ± 461 ng $m^{-3}$ (range: 10−2127 ng $m^{-3}$, Table 2) during the whole campaign, followed by methylglyoxal (mGly), succinin acid ($C_4$), terephthalic acid (tPh), and glyoxal (Gly). These five species account for 43%, 10%, 9%, 6% and 6% of total detected organic compounds (TDOC), respectively (Fig. 3).

As see in Fig. 4, TDOC in $PM_{2.5}$ are 1099 ± 1104, 325 ± 220 and 487 ± 387 ng $m^{-3}$ before-, during- and after-APEC, respectively. In comparison with those before-APEC, TDOC during-APEC decreased by 71%. Oxalic acid ($C_2$) is the leading species among the detected organic compounds and accounted for 46%, 31% and 34% of TDOC during the three phases, respectively (Fig. 4). $C_2$ is the end product of precursors that are photochemically oxidized in aerosol aqueous phase via either oxidation of small compounds containing two carbon atoms or decomposition of larger compounds containing three or more carbon atoms. Thus mass ratio of

Atmos. Chem. Phys. Discuss., doi:10.5194/acp-2016-662, 2016
Manuscript under review for journal Atmos. Chem. Phys.
Published: 22 August 2016
© Author(s) 2016. CC-BY 3.0 License.

Atmospheric Chemistry and Physics Discussions

$C_2$ to TDOC is indicative of aerosol aging (Wang et al., 2012; Ho et al., 2015). The highest proportion of $C_2$ before- APEC suggests that organic aerosols during this period are more oxidized. Glyoxal (Gly) and methylglyoxal (mGly) are the precursors of $C_2$. Mass ratios of both compounds to TDOC are lowest before-APEC and highest during-APEC (Fig. 4). In comparison with those before-APEC the decreased ratio $C_2$/TDOC and increased ratios of Gly/TDOC and mGly/TDOC during- and after-APEC, together with a decreased ratio of WSOC/OC discussed previously, further suggest a reducing production of SOA during the whole campaign.

### 3.3 Formation mechanism of oxalic acid

#### 3.3.1 Correlation of oxalic acid with temperature, relative humidity (RH), aerosol liquid water content (ALWC), acidity (pH), and sulfate

A few studies have pointed out that aerosol aqueous phase oxidation is a major formation pathway for oxalic acid (Yu et al., 2005; Pinxteren, et al., 2014; Bikkina et al., 2015; Tilgner et al, 2010). To explore the formation mechanism of oxalic acid, we calculated ALWC and pH of $PM_{2.5}$ aerosols by using ISOROPPIA-II, a state-of-the-art thermodynamic model (Weber et al., 2016). As shown in Fig. 5, during the entire period $C_2$ showed a strong linear correlation with sulfate ($R^2$=0.70 Fig. 5a), which is consistent with those observed in Xi'an (Wang et al., 2012) and other Chinese cities (Yu et al, 2005). Previous studies on particle morphology showed that sulfate particles internally mixes with SOA in Beijing especially in humid haze days (Li et al., 2010, 2011), which probably indicates that they are formed via similar aqueous phase pathways. Moreover, a robust correlation was also found for $C_2$ with RH ($R^2$=0.64, Fig. 5b) and aerosol liquid water content (ALWC) ($R^2$=0.61, Fig. 5c), indicating that humid conditions are favorable for the aqueous phase formation of $C_2$, which is most likely due to an enhanced gas-to-aerosol

Atmos. Chem. Phys. Discuss., doi:10.5194/acp-2016-662, 2016
Manuscript under review for journal Atmos. Chem. Phys.
Published: 22 August 2016
© Author(s) 2016. CC-BY 3.0 License.

Atmospheric Chemistry and Physics Discussions

aqueous phase partitioning of the precursors (e.g., Gly and mGly) (Fu et al., 2008; Wang et al., 2015).

The $H^+$aer calculated by using the ISORROPIA-II model indicates the aerosol aqueous phase acidity. As seen in Fig. 5d, $H^+$aer correlated well with $SO_4^{2-}$ ($R^2$ = 0.58), probably suggesting that $SO_4^-$ is the key factor controlling the aerosol acidity. The linear fit slope (1.03) indicates that the sulfate during the study period mostly appeared as bisulfate. In addition, $H^+$aer shows a significant positive correlation with $C_2$ ($R^2$ = 0.84) (Fig. 5e), possibly due to the fact that acidic conditions are favorable for the formation of $C_2$ precursors. For example, Surratt et al (2007; 2010) found that aerosol acidity can promote the formation of biogenic SOA (BSOA) derived from isoprene oxidation such as 2-methylglyceric acid, Gly and mGly. These BSOA precursors can be further oxidized into $C_2$ (Meng et al., 2014; Wang et al., 2009).

It is noteworthy that there is a significant positive correlation ($R^2$ = 0.58, $p$<0.001) between the mass ratios of $C_2$/TDOC and ambient temperatures (Fig. 5f), which is similar to the results found by previous researches (Ho et al., 2007; Strader et al., 1999) and suggests that aerosols are more oxidized under higher temperature conditions (Erven et al, 2011; Carlton et al., 2009). Therefore, both $C_2$/TDOC ratios (31% versus 34%) and TDOC concentrations (278 ng $m^{-3}$ versus 426 ng $m^{-3}$) during- and after-APEC are lower than those before-APEC (Fig. 4) due to the lower temperature conditions (13 ± 2.6 °C, 7.0 ± 1.7 °C and 4.3 ± 1.3 °C before-, during- and after-APEC periods, respectively) (Table1). Such results indicate that the significant reduction in $PM_{2.5}$ during the APEC period is largely ascribed to the emission controls, but the favorable meteorological conditions (e.g., the lower temperatures) may also take an important role.

**3.3.2 Temporal variation in stable carbon isotopic composition of oxalic acid**

Atmos. Chem. Phys. Discuss., doi:10.5194/acp-2016-662, 2016
Manuscript under review for journal Atmos. Chem. Phys.
Published: 22 August 2016
© Author(s) 2016. CC-BY 3.0 License.

Atmospheric Chemistry and Physics Discussions

To further discuss the formation mechanism of $C_2$, we investigated the temporal variations in concentration and stable carbon isotopic composition of $C_2$ in the $PM_{2.5}$ samples (Fig. 6). Previous studies have demonstrated that Gly, mGly, glyoxylic acid ($\omega C_2$) and pyruvic acid (Pyr) are the precursors of $C_2$ (Carlton et al., 2006, 2007; Ervens and Barbara, 2004; Wang et al., 2012). Thus, higher mass ratios of $C_2$ to its precursors indicate that organic aerosols are more oxidized (Wang et al., 2010). As shown in Table 3, $\delta^{13}C$ of $C_2$ in this work positively correlated with the mass ratios of $C_2/\omega C_2$, $C_2$/mGly and TDOC/WSOC, demonstrating an enrichment of $\delta^{13}C$ during the aerosol oxidation process. Because decomposition (or breakdown) of larger molecular weight precursors in aerosol aqueous phase is the dominant formation pathway for $C_2$ in aerosol ageing process (Kawamura et al., 2016; Gensch et al., 2014; Kirillova et al., 2013), during which organic compounds release $CO_2$/CO by reaction with OH radical and other oxidants, resulting in the evolved species enriched with lighter isotope ($^{12}C$) and the remaining substrate enriched in $^{13}C$ due to kinetic isotope effects (KIEs) (Hoefs, 1997; Rudolph et al., 2002).

72-h backward trajectory analysis showed that air masses moved to Beijing during the whole sampling period can roughly be categorized into three types (Fig. 6a) (all trajectories during the entire study period can be found in the supplementary materials). (1) Regional type, by which air masses originated from inland and east coastal China and moved slowly into Beijing via a long distance within 72-h from its south regions, i.e., Henan, Shandong and Jiangsu provinces. Air pollution in the three provinces is severe, and thus aerosols transported by this type of air masses are of regional characteristics. (2) Local type, by which air masses originated from Mongolia and north China, and moved quickly into Hebei province and then turned back to Beijing. Air in Mongolia and north China is clean but is polluted in Hebei province, which is

Atmos. Chem. Phys. Discuss., doi:10.5194/acp-2016-662, 2016
Manuscript under review for journal Atmos. Chem. Phys.
Published: 22 August 2016
© Author(s) 2016. CC-BY 3.0 License.

Atmospheric Chemistry and Physics Discussions

adjacent to Beijing. Since the resident time of the air masses within Hebei province is very short, thus aerosols transported by this type of air masses is of local characteristics and relatively fresh. (3) Long-range transport type, by which air masses originated from Siberia and moved rapidly into Beijing directly by a long-range transport. Aerosols from the long-range transport type air masses are much more aged, while those from the local type air masses are fresh. Since severe air pollution is widespread in the south regions, gas-to-aerosol phase partitioning of precursors and subsequent aerosol-phase oxidation to produce SOA including $C_2$ continuously proceed during the air mass movement. However, such a partition for producing SOA is not significant when air mass move from Mongolia, north China and Siberia, because of the much less abundant VOCs. In stead, aerosols in the north air masses are continuously oxidized, during which $C_2$ is produced by photochemical decomposition of larger molecular weight precursors. Therefore, $C_2$ in $PM_{2.5}$ transported by the local type air masses are not only fresh and abundant but also enriched in $^{12}C$, whereas $C_2$ in $PM_{2.5}$ transported by the long-range transport type air masses are aged, less abundant and enriched in $^{13}C$ due to KIE effects, as exemplified by the pink and light blue columns in Fig. 6b, respectively. $C_2$ in $PM_{2.5}$ transported by the regional type air masses are most abundant compared with that in other two type of air masses, which is not only due to the severe air pollution in the Henan, Shandong and Jiangsu provinces but also due to the enhanced photochemical oxidation under the humid and higher temperature conditions that occurred mostly before-APEC, as discussed previously. Therefore, $C_2$ in the regional type air masses is not only abundant but also enriched in $^{13}C$ (see black columns in Fig. 6b)

### 3.4 Different chemical characteristics of $PM_{2.5}$ between two serve haze events

Atmos. Chem. Phys. Discuss., doi:10.5194/acp-2016-662, 2016
Manuscript under review for journal Atmos. Chem. Phys.
Published: 22 August 2016
© Author(s) 2016. CC-BY 3.0 License.

Atmospheric Chemistry and Physics Discussions

316 From Fig. 1 and Table 4, it can be found that $PM_{2.5}$ showed two equivalent maxima on 9$^{th}$
317 October and 20$^{th}$ November during the whole study period. However, the chemical compositions
318 of $PM_{2.5}$ during these two pollution events were significantly different. As shown in Fig. 7a,
319 relative abundances of SIA (sum of $SO_4^{2-}$+$NO_3^-$+$NH_4^+$) to $PM_{2.5}$ are 30% during the event I and
320 23% during the event II, respectively. The relative abundance of OM (21%, Fig. 7a) during the
321 event I is lower than that (37%) during the event II, but the ratios of WSOC/OC and TDOC/OC
322 are higher in the event I than in event II (Fig. 7b). Organic biomarkers in the $PM_{2.5}$ have been
323 measured for the source apportionment (Wang et al., 2016) and citied here to further identify the
324 difference in chemical composition of $PM_{2.5}$ between the two events. Levoglucosan is a key
325 tracer for biomass burning smoke. Mass ratio of levoglucosan to OC in $PM_{2.5}$ (Lev/OC) is
326 comparable between the two events, suggesting a similar level of contributions of biomass
327 burning emission to $PM_{2.5}$ before- and after-APEC. However, the mass ratios of PAHs and
328 hopanes to OC are lower in event I than those in event II (Fig. 7c), which again demonstrate the
329 enhanced emissions from coal burning for house heating, because these compounds are key
330 tracers of coal burning smokes (Wang et al., 2006). As seen in Fig. 7d, $C_2$ in the event I was
331 more enriched in $\delta^{13}C$. Such relatively more abundant SIA, WSOC and TDOC and heavier $C_2$ in
332 $PM_{2.5}$ clearly demonstrate that $PM_{2.5}$ during the event I were enriched with secondary products
333 while the fine particles during the event II were enriched with primary compounds. After-APEC
334 house heating activities including residential coal burning were activated, which emited huge
335 amounts of $SO_2$, NOx, and VOCs as well as primary particles. For example, Li et al (2015)
336 found VOCs at the urban center of Beijing rapidly increased from 48.28 ppbv during-APEC to
337 72.97 ppbv after-APEC. However, the lower temperature after-APEC is unfavorable for

Atmos. Chem. Phys. Discuss., doi:10.5194/acp-2016-662, 2016
Manuscript under review for journal Atmos. Chem. Phys.
Published: 22 August 2016
© Author(s) 2016. CC-BY 3.0 License.

Atmospheric Chemistry and Physics Discussions

photochemical oxidation, thus resulting in secondary aerosol production much less abundant compared with those before-APEC. Temperatures during-APEC were also lower than those before-APEC. Thus, compared to those before-APEC the much lower $PM_{2.5}$ levels during-APEC were caused not only by the emission controls but also by the lower temperatures.

## 4. Summary and conclusion

Temporal variations in molecular distribution of SIA, dicarboxylic acids, ketoacids and α-dicarbonyl and stable carbon isotopic composition ($\delta^{13}C$) of $C_2$ in $PM_{2.5}$ collected in Beijing before-, during- and after- the 2014 APEC were investigated. Absolute concentrations and relative abundances of SIA and $C_2$ in $PM_{2.5}$ are highest before-APEC, followed by those after- and during-APEC, suggesting that the fine aerosols before-APEC are enriched with secondary products, mainly due to an enhanced photochemical oxidation under the higher temperature and RH conditions. Concentrations of SIA, oxalic acid and related SOA in $PM_{2.5}$ during-APEC are 2−4 times lower than those before-APEC, which is not only due to the effective emission controls but also due to the lower temperature conditions that are unfavorable for secondary aerosol production.

Positive correlations of $C_2$ with RH, sulfate mass, ALWC and aerosol acidity indicate that $C_2$ formation pathway is involved an acid-catalyzed aerosol aqueous phase oxidation. SIA, $C_2$ and related SOA in the regional air masses are abundant with $C_2$ enriched in $^{13}C$. On the contrary, those in the long-range transport air masses are much less abundant, although $C_2$ is also enriched in $^{13}C$. By comparing the chemical composition of $PM_{2.5}$ and $\delta^{13}C$ values of $C_2$ in two events that are characterized by two highest values of $PM_{2.5}$ before- and after-APEC, we further found that compared with those before- APEC fine aerosols after-APEC are enriched with primary species

© Author(s) 2016. CC-BY 3.0 License.

and $C_2$ is depleted in heavier $^{13}C$, although $SO_2$, NOx and VOCs are much more abundant during the heating season, again demonstrating the important role of temperature in secondary aerosol production that is enhanced before-APEC and reduced during-APEC. Therefore, compared with that before APEC the significant reduction of $PM_{2.5}$ during-APEC is firstly ascribed to the stringent emission controls and secondly attributed to the lower temperatures that suppressed secondary aerosol production.

**Acknowledgements**

This work was financially supported by the Strategic Priority Research Program of the Chinese Academy of Sciences (Grants No. XDB05020401 and XDA05100103), the China National Natural Science Founds for Distinguished Young Scholars (Grants No. 41325014), and the program from National Nature Science Foundation of China (No. 41405122, 91544226 and 41375132 ).

**References**

Bikkina, S., Kawamura, K., and Miyazaki, Y.: Latitudinal distributions of atmospheric dicarboxylic acids, oxocarboxylic acids, and α-dicarbonyls over the western North Pacific: Sources and formation pathways, Journal of Geophysical Research: Atmospheres, 120, 5010-5035, 10.1002/2014jd022235, 2015.

Carlton, A. G., Turpin, B. J., Lim, H.-J., Altieri, K. E., and Seitzinger, S.: Link between isoprene and secondary organic aerosol (SOA): Pyruvic acid oxidation yields low volatility organic acids in clouds, Geophysical Research Letters, 33, 10.1029/2005gl025374, 2006.

Carlton, A. G., Turpin, B. J., Altieri, K. E., Seitzinger, S., Reff, A., Lim, H.-J., and Ervens, B.: Atmospheric oxalic acid and SOA production from glyoxal: Results of aqueous photooxidation experiments, Atmos. Environ., 41, 7588-7602, 2007.

Carlton, A., Wiedinmyer, C., and Kroll, J.: A review of Secondary Organic Aerosol (SOA) formation from isoprene, Atmos. Chem. Phy., 9, 4987-5005, 2009.

Cheng, C., Wang, G., Meng, J., Wang, Q., Cao, J., Li, J., and Wang, J.: Size-resolved airborne particulate oxalic and related secondary organic aerosol species in the urban atmosphere of Chengdu, China, Atmospheric Research, 161-162, 134-142, 10.1016/j.atmosres.2015.04.010, 2015.

Chow, J. C., Watson, J. G., Chen, L.-W. A., Chang, M. O., Robinson, N. F., Trimble, D., and Kohl, S.: The IMPROVE_A temperature protocol for thermal/optical carbon analysis: maintaining consistency with a long-term database, Journal of the Air & Waste Management Association, 57, 1014-1023, 2007.

Ervens, B.: A modeling study of aqueous production of dicarboxylic acids: 1. Chemical pathways and speciated organic mass production, J. Geophys. Res., 109, 10.1029/2003jd004387, 2004.

Ervens, B., Turpin, B. J., and Weber, R. J.: Secondary organic aerosol formation in cloud droplets and aqueous particles (aqSOA): a review of laboratory, field and model studies, Atmos. Chem. Phys., 11, 11069-11102, 2011.

© Author(s) 2016. CC-BY 3.0 License.

Fu, T.-M., Jacob, D. J., Wittrock, F., Burrows, J. P., Vrekoussis, M., and Henze, D. K.: Global budgets of atmospheric glyoxal and methylglyoxal, and implications for formation of secondary organic aerosols, J. Geophys. Res., 113, D15303,doi:15310.11029/12007JD009505, 2008.

Gao, S., Ng, N. L., Keywood, M., Varutbangkul, V., Bahreini, R., Nenes, A., He, J., Yoo, K. Y., Beauchamp, J. L., Hodyss, R. P., Flagan, R. C., and Seinfeld, J. H.: Particle phase acidity and oligomer formation in secondary organic aerosol, Environ. Sci. Technol., 38, 6582-6589, 2004.

Gensch, I., Kiendler-Scharr, A., and Rudolph, J.: Isotope ratio studies of atmospheric organic compounds: Principles, methods, applications and potential, International Journal of Mass Spectrometry, 365-366, 206-221, 10.1016/j.ijms.2014.02.004, 2014.

Guo, S., Hu, M., Zamora, M. L., Peng, J., Shang, D., Zheng, J., Du, Z., Wu, Z., Shao, M., Zeng, L., Molina, M. J., and Zhang, R.: Elucidating severe urban haze formation in China, Proceedings of the National Academy of Sciences, 111(49), 17373-17378, 2014.

Ho, K. F., Cao, J. J., Lee, S. C., Kawamura, K., Zhang, R. J., Chow, J. C., and Watson, J. G.: Dicarboxylic acids, ketocarboxylic acids, and dicarbonyls in the urban atmosphere of China, J. Geophys. Res., 112, 10.1029/2006jd008011, 2007.

Ho, K. F., Lee, S. C., Ho, S. S. H., Kawamura, K., Tachibana, E., Cheng, Y., and Zhu, T.: Dicarboxylic acids, ketocarboxylic acids,α-dicarbonyls, fatty acids, and benzoic acid in urban aerosols collected during the 2006 Campaign of Air Quality Research in Beijing (CAREBeijing-2006), J. Geophys. Res., 115, 10.1029/2009jd013304, 2010.

Ho, K. F., Huang, R. J., Kawamura, K., Tachibana, E., Lee, S. C., Ho, S. S. H., Zhu, T., and Tian, L.: Dicarboxylic acids, ketocarboxylic acids, α-dicarbonyls, fatty acids and benzoic acid in $PM_{2.5}$ aerosol collected during CAREBeijing-2007: an effect of traffic restriction on air quality, Atmospheric Chemistry and Physics, 15, 3111-3123, 10.5194/acp-15-3111-2015, 2015.

Hoefs, J., *Stable Isotope Geochemistry.*, Springer, New York, 1997.

Huang, R. J., Zhang, Y., Bozzetti, C., Ho, K. F., Cao, J. J., Han, Y., Daellenbach, K. R., Slowik, J. G., Platt, S. M., Canonaco, F., Zotter, P., Wolf, R., Pieber, S. M., Bruns, E. A., Crippa, M., Ciarelli, G., Piazzalunga, A., Schwikowski, M., Abbaszade, G., Schnelle-Kreis, J., Zimmermann, R., An, Z., Szidat, S., Baltensperger, U., El Haddad, I., and Prevot, A. S.: High secondary aerosol contribution to particulate pollution during haze events in China, Nature, 514, 218-222, 10.1038/nature13774, 2014.

Kawamura, K., and Watanabe, T.: Determination of stable carbon isotopic compositions of low molecular weight dicarboxylic acids and ketocarboxylic acids in atmospheric aerosol and snow samples, Analytical Chemistry, 76, 5762-5768, 2004.

Kawamura, K., and Bikkina, S.: A review of dicarboxylic acids and related compounds in atmospheric aerosols: Molecular distributions, sources and transformation, Atmospheric Research, 10.1016/j.atmosres.2015.11.018, 2015.

Kirillova, E. N., Andersson, A., Sheesley, R. J., Kruså, M., Praveen, P. S., Budhavant, K., Safai, P. D., Rao, P. S. P., and Gustafsson, Ö.: $^{13}C$- and$^{14}C$-based study of sources and atmospheric processing of water-soluble organic carbon (WSOC) in South Asian aerosols, J. Geophys. Res., 118, 614-626, 2013.

Li, J., Xie, S. D., Zeng, L. M., Li, L. Y., Li, Y. Q., and Wu, R. R.: Characterization of ambient volatile organic compounds and their sources in Beijing, before, during, and after Asia-Pacific Economic Cooperation China 2014, Atmos. Chem. Phys., 15, 7945-7959, 2015.

Li, W.J. and Shao, L.Y.: Mixing and water-soluble characteristics of particulate organic compounds in individual urban aerosol particles. J. Geophys. Res. 115 (D02301), doi:10.1029/2009JD012575, 2010.

© Author(s) 2016. CC-BY 3.0 License.

440 Li, W.J., Zhou, S.Z., Wang, X.F., Xu, Z., Yuan, C., Yu, Y.C., Zhang, Q.Z. and Wang, W.X.: Integrated evaluation
441 of aerosols from regional brown hazes over northern China in winter: Concentrations, sources, transformation,
442 and mixing states. J. Geophys. Res. 116 (D9), doi:10.1029/2010JD015099,2011.
443 Laskin, A., Laskin, J., and Nizkorodov, S. A.: Chemistry of atmospheric brown carbon, Chem. Rev., 115,
444 4335-4382, 2015.
445 Meng, J., Wang, G., Li, J., Cheng, C., Ren, Y., Huang, Y., Cheng, Y., Cao, J., and Zhang, T.: Seasonal
446 characteristics of oxalic acid and related SOA in the free troposphere of Mt. Hua, central China: implications for
447 sources and formation mechanisms, Sci Total Environ, 493, 1088-1097, 2014.
448 Mu Quan, Z. S.: An evaluation of the economic loss due to the heavy haze during January 2013 in China., China
449 Environmental Science, 33, 2087-2094, 2013.
450 Pathak, R. K., Wang, T., Ho, K. F., and Lee, S. C.: Characteristics of summertime PM2.5 organic and elemental
451 carbon in four major Chinese cities: Implications of high acidity for water-soluble organic carbon (WSOC),
452 Atmos. Environ., 45, 318-325, 10.1016/j.atmosenv.2010.10.021, 2011.
453 Rudolph, J., Czuba, E., Norman, A., Huang, L., and Ernst, D.: Stable carbon isotope composition of nonmethane
454 hydrocarbons in emissions from transportation related sources and atmospheric observations in an urban
455 atmosphere, Atmos. Environ., 36, 1173-1181, 2002.
456 Strader, R., Lurmann, F., and Pandis, S. N.: Evaluation of secondary organic aerosol formation in winter, Atmos.
457 Environ., 33, 4849-4863, 1999.
458 Sullivan, R. C., and Prather, K. A.: Investigations of the diurnal cycle and mixing state of oxalic acid in individual
459 particles in Asian aerosol outflow, Environ. Sci. Technol., 41, 8062-8069, 2007.
460 Sun, Y., Wang, Z., Wild, O., Xu, W., Chen, C., Fu, P., Du, W., Zhou, L., Zhang, Q., Han, T., Wang, Q., Pan, X.,
461 Zheng, H., Li, J., Guo, X., Liu, J., and Worsnop, D. R.: "APEC Blue": Secondary Aerosol Reductions from
462 Emission Controls in Beijing, Scientific reports, 6, 20668, 10.1038/srep20668, 2016.
463 Surratt, J. D., Lewandowski, M., Offenberg, J. H., Jaoui, M., Kleindienst, T. E., Edney, E. O., and Seinfeld, J. H.:
464 Effect of Acidity on Secondary Organic Aerosol Formation from Isoprene, Environ. Sci. Technol., 41,
465 5363-5369, 2007.
466 Surratt, J. D., Chan, A. W. H., Eddingsaas, N. C., Chan, M., Loza, C. L., Kwan, A. J., Hersey, S. P., Flagan, R. C.,
467 Wennberg, P. O., and Seinfeld, J. H.: Reactive intermediates revealed in secondary organic aerosol formation
468 from isoprene, Proceedings of National Academy of Science of United States of America, 107, 6640-6645,
469 2010.
470 Tang, G., Zhu, X., Hu, B., Xin, J., Wang, L., Münkel, C., Mao, G., and Wang, Y.: Impact of emission controls on
471 air quality in Beijing during APEC 2014: lidar ceilometer observations, Atmos. Chem. Phys., 15, 12667-12680,
472 2015.
473 Tilgner, A. and Herrmann, H.: Radical-driven carbonyl-to-acid conversion and acid degradation in tropospheric
474 aqueous systems studied by CAPRAM. Atmos. Environ., 44, 5415-5422, 2010.
475 Van Donkelaar, A., Martin, R. V., Brauer, M., Kahn, R., Levy, R., Verduzco, C., and Villeneuve, P. J.: Global
476 estimates of ambient fine particulate matter concentrations from satellite-based aerosol optical depth:
477 development and application, University of British Columbia, 2015.
478 van Pinxteren, D., Neusüß, C., and Herrmann, H.: On the abundance and source contributions of dicarboxylic acids
479 in size-resolved aerosol particles at continental sites in central Europe, Atmos. Chem. Phys., 14, 3913-3928,
480 2014.
481 Wang, G., Cheng, C., Meng, J., Huang, Y., Li, J. and Ren, Y.: Field observation on secondary organic aerosols
482 during Asian dust storm periods: Formation mechanism of oxalic acid and related compounds on dust surface.
483 Atmos. Environ., 113, 169-176, 2015.

© Author(s) 2016. CC-BY 3.0 License.

484 Wang, G. H., Kawamura, K., Lee, S. C., Ho, K. F. and Cao, J. J.: Molecular, seasonal and spatial distributions of
485 organic aerosols from fourteen Chinese cities. Environ. Sci. Technol., 40, 4619-4625, 2006.
486 Wang, G., Kawamura, K., Umemoto , N., Xie, M., Hu, S. and Wang, Z.: Water-soluble organic compounds in
487 PM2.5 and size-segregated aerosols over Mt. Tai in North China Plain. Journal of Geophysical
488 Research-Atmospheres, 114, D19208, dio.10.1029/2008JD011390, 2009.
489 Wang, G., Kawamura, K., Cheng, C., Li, J., Cao, J., Zhang, R., Zhang, T., Liu, S., and Zhao, Z.: Molecular
490 distribution and stable carbon isotopic composition of dicarboxylic acids, ketocarboxylic acids, and
491 alpha-dicarbonyls in size-resolved atmospheric particles from Xi'an City, China, Environ. Sci. Technol., 46,
492 4783-4791, 2012.
493 Wang, G., Xie, M., Hu, S., Gao, S., Tachibana, E., and Kawamura, K.: Dicarboxylic acids, metals and isotopic
494 compositions of C and N in atmospheric aerosols from inland China: implications for dust and coal burning
495 emission and secondary aerosol formation, Atmos. Chem. Phys., 10, 6087-6096, 2010.
496 Wang, G., Wang, J., Ren, Y. and Li, J.: Chemical characterization of organic aerosols from Beijing during the 2014
497 APEC (under preparation), 2016.
498 Wang, Y., Zhang, Q. Q., He, K., Zhang, Q., and Chai, L.: Sulfate-nitrate-ammonium aerosols over China: response
499 to 2000–2015 emission changes of sulfur dioxide, nitrogen oxides, and ammonia, Atmos. Chem. Phys., 13,
500 2635-2652, 2013.
501 Weber, R. J., Guo, H., Russell, A. G., and Nenes, A.: High aerosol acidity despite declining atmospheric sulfate
502 concentrations over the past 15 years, Nature Geoscience, 9, 282-285, 10.1038/ngeo2665, 2016.
503 Xing, L., Fu, T. M., Cao, J. J., Lee, S. C., Wang, G. H., Ho, K. F., Cheng, M. C., You, C. F., and Wang, T. J.:
504 Seasonal and spatial variability of the OM/OC mass ratios and high regional correlation between oxalic acid and
505 zinc in Chinese urban organic aerosols, Atmos. Chem. Phys., 13, 4307-4318, 2013.
506 Xu, W. Q., Sun, Y. L., Chen, C., Du, W., Han, T. T., Q.Wang, Q., Fu, P. Q., F.Wang, Z., Zhao, X. J., Zhou, L. B., Ji,
507 D. S., Wang, P. C., and Worsnop, D. R.: Aerosol composition, oxidation properties, and sources in Beijing:
508 results from the 2014 Asia-Pacific Economic Cooperation summit study, Atmos. Chem. Phys., 15, 13681–13698,
509 2015.
510 Yu, J. Z., Huang, X.-F., Xu, J., and Hu, M.: When Aerosol Sulfate Goes Up, So Does Oxalate: Implication for the
511 Formation Mechanisms of Oxalate, Environ. Sci. Technol., 39, 128-133, 2005.
512 Zhang, Q., Jimenez, J. L., Worsnop, D. R., and Canagaratna, M.: A case study of urban particle acidity and its
513 influence on secondary organic aerosol, Environ. Sci. Technol., 41, 3213-3219, 2007.
514 Zhang, Q., Streets, D. G., Carmichael, G. R., He, K., Huo, H., Kannari, A., Klimont, Z., Park, I., Reddy, S., and Fu,
515 J.: Asian emissions in 2006 for the NASA INTEX-B mission, Atmos. Chem. Phys., 9, 5131-5153, 2009.
516 Zhang, R., Wang, G., Guo, S., Zamora, M. L., Ying, Q., Lin, Y., Wang, W., Hu, M., and Wang, Y.: Formation of
517 urban fine particulate matter, Chemical Reviews, 115, 3803-3855, 2015.
518 Zheng, G. J., Duan, F. K., Su, H., Ma, Y. L., Cheng, Y., Zheng, B., Zhang, Q., Huang, T., Kimoto, T., Chang, D.,
519 Pöschl, U., Cheng, Y. F., and He, K. B.: Exploring the severe winter haze in Beijing: the impact of synoptic
520 weather, regional transport and heterogeneous reactions, Atmos. Chem. Phys., 15, 2969-2983, 2015.

521

Atmos. Chem. Phys. Discuss., doi:10.5194/acp-2016-662, 2016
Manuscript under review for journal Atmos. Chem. Phys.
Published: 22 August 2016
© Author(s) 2016. CC-BY 3.0 License.

Atmospheric Chemistry and Physics Discussions

## Figure Captions

**Figure 1.** Temporal variations of meteorological conditions, gaseous pollutants and major components of $PM_{2.5}$ during the 2014 APEC campaign. (The brown shadows represent two air pollution events characterized by highest $PM_{2.5}$ levels before- and after-APEC, while the blue shadow represents the APEC event).

**Figure 2.** Chemical composition of $PM_{2.5}$ during the 2014 APEC campaign.

**Figure 3**. Molecular distributions of dicarboxylic acids and related compounds in $PM_{2.5}$ of Beijing, China during the 2014 APEC campaign. The pie chart is the average composition of total detected organic compounds (TDOC) and the top number is the average mass concentration of TDOC of the whole study period.

**Figure 4**. Compositions of total detected organic compounds (TDOC) in $PM_{2.5}$ during the 2014 APEC campaign.

**Figure 5.** Correlation analysis for oxalic acid ($C_2$) and sulfate in $PM_{2.5}$ during the whole 2014 APEC campaign. (**a-c**) Concentrations of $C_2$ with sulfate, relative humidity (RH), and aerosol liquid water content (ALWC); (**d, e**) sulfate and $C_2$ with aerosol acidity [$H^+$] and (**f**) temperature with mass ratio of $C_2$ to total detected organic compounds ($C_2$/TDOC).

**Figure 6**. (**a**) 72-h backward trajectories determined by the National Oceanic and Atmospheric Administration Hybrid Single Particle Lagrangian Integrated Trajectory (HYSPLIT) model arriving at the sampling site to reveal the major air mass flow types during the study period. Northwesterly wind (light blue) was most frequently (64%), followed by northerly (21%, pink) and southerly (15%, black) and is defined as long-range transport, local and regional type, respectively (see the definitions in the text); (**b**) Time series of $\delta^{13}C$ values and concentration of oxalic acid during the whole study period (Colors in Fig. 6a are corresponding to those in Fig. 6b).

**Figure 7.** Comparison of chemical composition of $PM_{2.5}$ during two air pollution events.(**a**) Percentages of major species in $PM_{2.5}$; (**b,** c) mass ratios of major species and organic tracers in $PM_{2.5}$; (**d**) stable carbon isotope composition of oxalic acid ($C_2$) (Data about levoglucosan (Lev), PAHs and hopanes are cited from Wang et al (2016)).

Atmos. Chem. Phys. Discuss., doi:10.5194/acp-2016-662, 2016
Manuscript under review for journal Atmos. Chem. Phys.
Published: 22 August 2016
© Author(s) 2016. CC-BY 3.0 License.

Atmospheric Chemistry and Physics Discussions

559
560
561
562
563
564
565
566
567
568
569
570
571
572
573
574
575
576
577
578
579
580
581
582
583
584
585

Table 1. Meteorological parameters and concentrations (μg $m^{-3}$) of gaseous pollutants and chemical components of $PM_{2.5}$ in Beijing during the 2014 APEC campaign

| | Whole period (N=48) | Before-APEC (08/10−02/11) (N=26) | During-APE (03/11−12/11) (N=10) | After-APEC (13/11−14/11) (N=12) |
|---|---|---|---|---|
| I. Meteorological parameters | | | | |
| Temperature, °C | 9.5± 4.3 (3.0−18) | 13±2.6 (9.0−18) | 7.0±1.7 (4.0−10) | 4.3±1.3 (3.0−7.0) |
| Relative humidity, % | 56±19 (17−88) | 62±19 (22−88) | 47±14 (17−65) | 51±16 (29−80) |
| Visibility, km | 8.8±6.8 (1.0−28) | 7.3±6.6 (1.0−24) | 13±7.7 (6.0−28) | 7.2±4.2 (2.0−15) |
| Wind speed, km $h^{-1}$ | 8.0±4.9 (3.0−26) | 7.6±4.8 (3.0−26) | 9.4±6.6 (3.0−26) | 7.8±2.9 (3.0−13) |
| II. Gaseous pollutants | | | | |
| $O_3$ | 48 ± 23 (6.0−115) | 55 ± 24 (9.0−115) | 52 ± 13 (25−69) | 29 ± 18 (6.0−60) |
| $SO_2$ | 12 ± 8.5 (2.0−43) | 8.8 ± 4.6 (2.0−19) | 7.6 ± 3.9 (2.0−15) | 23 ± 8.8 (13−43) |
| $NO_2$ | 68±29 (10−135) | 71 ± 27 (22−118) | 45 ± 18 (10−69) | 78 ± 29 (45−135) |
| III. Major components of $PM_{2.5}$ | | | | |
| $PM_{2.5}$ | 157 ± 110 (16−408) | 178 ± 122 (16−408) | 98 ± 46 (28−183) | 161 ± 100 (36−383) |
| $SO_4^{2-}$ | 12 ± 11.5 (1.2−43) | 15 ± 13 (1.2−43) | 5.3 ± 2.8 (1.8−11) | 11 ±10 (2.9−34) |
| $NO_3^-$ | 21 ± 22 (0.32−88) | 28 ± 26 (0.32−88) | 10 ±8.1 (1.2−26) | 15 ± 13 (2.9−46) |
| $NH_4^+$ | 7.3± 7.2 (0.2−28) | 9.0 ± 8.0 (0.21−28) | 3.1 ± 2.6 (0.2−8.6) | 6.9 ± 6.4 (1.0−22) |
| OC | 28 ± 18 (5.7−78) | 26 ± 16 (6.0−67) | 19 ± 7.6 (5.7−29) | 39 ± 23 (9.7−78) |
| EC | 8.8 ± 5.4 (1.4−25) | 8.6 ± 4.6 (1.4−18) | 6.0 ± 2.7 (1.5−9.6) | 12 ± 7.0 (2.1−25) |
| WSOC | 10 ± 6 (2.4−32) | 11± 4.6 (3.1−32) | 6.4 ± 2.6 (2.4−11) | 11 ± 6.1 (4.5−24) |
| $NO_3^-/SO_4^{2-}$ | 1.6±0.8 (0.3−4.3) | 1.7±0.9 (0.3−4.3) | 1.6±0.7 (0.5−2.4) | 1.4±0.4 (0.8−2.2) |
| OC/EC | 3.3±0.6 (2.2−4.7) | 3.2±0.7 (2.2−4.5) | 3.3±0.6 (2.0−4.3) | 3.4±0.5 (2.7−4.7) |
| WSOC/OC | 0.39±0.15 (0.10−0.71) | 0.42±0.13 (0.13−0.71) | 0.38±0.16 (0.16−0.65) | 0.35±0.17 (0.10−0.63) |

Atmos. Chem. Phys. Discuss., doi:10.5194/acp-2016-662, 2016
Manuscript under review for journal Atmos. Chem. Phys.
Published: 22 August 2016
© Author(s) 2016. CC-BY 3.0 License.

Atmospheric Chemistry and Physics Discussions

586
587

Table 2. Concentrations of dicarboxylic acids and related compounds in $PM_{2.5}$ in Beijing during the 2014 APEC campaign (ng $m^{-3}$)

| | Whole period (N=48) | Before-APEC (08/10−02/11) (N=26) | During-APE (03/11−12/11) (N=10) | After-APEC (13/11−14/11) (N=12) |
|---|---|---|---|---|
| | | I. Dicarboxylic acids | | |
| Oxalic, $C_2$ | 334 ± 461 (10−2127) | 502 ± 564 (10.5−2127) | 101 ± 69 (35−251) | 166 ± 157 (22−554) |
| Malonic, $C_3$ | 31 ± 42 (ND−247) | 45.7 ± 52.1 (1.44−247) | 12 ± 8.0 (3.4−22.8) | 16± 10.9 (ND−36) |
| Succinic, $C_4$ | 74 ± 118 (3.0−722) | 111 ± 150 (3.0−722) | 24 ± 14 (7.1−42) | 36 ± 26 (4.9−90) |
| Glutaric, $C_5$ | 8.7 ± 12 (ND−68) | 13± 15 (ND−68.1) | 2.9 ± 2.24 (0.9−5.8) | 4.9 ± 4.2 (ND−13) |
| Adipic, $C_6$ | 13± 14 (0.9−83) | 17 ± 18 (1.9−83) | 5.9 ±3.8 (2.1−14) | 9.9 ± 7.1 (2.0−23) |
| Pimelic, $C_7$ | 2.1 ± 3.8 (ND−27) | 2.6 ± 5.1(ND−27) | 1.1 ± 0.7(0.2−2.3) | 2.0 ± 1.1 (0.9−4.4) |
| Suberic, $C_8$ | 10 ± 11 (ND−66) | 12± 13 (ND−66) | 7.6 ± 5.0 (1.3−16) | 8.7 ± 6.0(2.0−21) |
| Azelaic, $C_9$ | 5.0± 4.9(0.5−21) | 6.4 ± 5.7 (0.6−21) | 1.7± 0.9 (0.5−3.2) | 4.6 ± 3.3 (1.3−13) |
| Sebacic, $C_{10}$ | 7.7 ± 7.4 (ND−34) | 9.4 ± 8.8 (ND−34) | 4.2± 3.6 (0.5−11) | 6.8 ± 4.9 (1.4−16) |
| Undecanedioic, $C_{11}$ | 11 ± 13 (ND−77) | 14 ± 16 (ND−77) | 3.3 ± 2.5 (ND−7.5) | 9.4 ± 6.4 (0.8−23) |
| Methylsuccinic, $iC_5$ | 13 ± 16 (0.6−79) | 18 ± 19 (0.6−79) | 4.8 ± 3.0 (1.0−9.2) | 8.4 ± 6.0(2.3−19) |
| Methyglutaric, $iC_6$ | 7.5 ± 10 (ND−36) | 11± 12 (ND−36) | 0.9 ± 09 (ND−2.6) | 4.6± 5.1 (ND−14) |
| Maleic, M | 3.4 ± 3.9 (ND−15) | 4.6± 4.7 (ND−15) | 1.4 ± 0.8 (ND−2.9) | 2.4 ± 2.0 (ND−6.3) |
| Fumaric, F | 7.2 ± 8.8 (ND−64) | 10 ± 11 (ND−64) | 2.2 ± 1.5 (ND−5.4) | 4.7 ± 3.2 (1.4−10) |
| Phthalic, Ph | 17 ± 14 (1.5−64) | 20 ± 16 (1.5−64) | 10 ± 6.8 (2.3−20) | 17 ± 9.0 (6.4−31) |
| Isophthalic, iPh | 2.1 ± 2.5 (ND−10) | 2.9 ± 2.8 (ND−10) | 2.0 ± 2.1 (0.2−5.9) | 0.5 ± 0.3 (ND−3.2) |
| Terephthalic, tPh | 46 ± 35 (2.6−133) | 50 ± 35 (2.6−123) | 28 ± 19(4.7−59) | 53± 40 (7.4−133) |
| Subtotal | 593 ± 739 (25−3788) | 849 ± 905 (25−3788) | 214 ± 135 (72−447) | 354 ± 279 (85−965) |
| | | II. Keto-carboxylic acids | | |
| Pyruvic, Pyr | 24 ± 20 (1.3−84) | 31± 23 (2.4−84) | 15 ± 12 (1.3−36) | 15 ± 9.3 (3.2−33) |
| Glyoxylic, $\omega C_2$ | 33 ± 51 (1.2−300) | 48± 64 (1.2−300) | 10 ± 7.7 (2.6−21) | 20 ± 23 (2.8−80) |
| 7-Oxoheptanoic, $\omega C_7$ | 8.8 ± 14 (ND−90) | 13 ± 17 (ND−90) | 4.2 ± 3.6 (ND−13) | 4.5 ± 5.1 (ND−17) |
| Subtotal | 66 ± 81 (3.6−474) | 92 ± 99 (3.6−474) | 30 ± 22 (5.9−66) | 40 ± 35 (13−128) |
| | | III α-Dicarbonyls | | |
| Glyoxal, Gly | 44 ± 47 (4.2−270) | 57 ± 56 (4.2−270) | 22 ± 19 (4.9−47) | 35 ± 30 (7.3−101) |
| Methylglyoxal, mGly | 82 ± 82 (ND−406) | 102 ± 96 (ND−406) | 60 ± 52 (15−139) | 58 ± 51 (5.8−144) |
| Subtotal | 126 ± 115 (5.3−466) | 158 ± 132 (5.3−466) | 81.6 ± 67.4 (22−186) | 93 ± 80 (14−225) |
| TDOC[b] | 785 ± 872 (36−4636) | 1099 ± 1104 (36−4636) | 325 ± 220 (107−664) | 487 ± 387 (117-1318) |

[a]ND: not detectable; [b]TDOC: total detected organic compounds.

Atmos. Chem. Phys. Discuss., doi:10.5194/acp-2016-662, 2016
Manuscript under review for journal Atmos. Chem. Phys.
Published: 22 August 2016
© Author(s) 2016. CC-BY 3.0 License.

Atmospheric Chemistry and Physics Discussions

588
589
590

Table 3 Linear correlation coefficients of $\delta^{13}C$ of $C_2$ with $C_2/\omega C_2$, $C_2$/mGly, and TDOC/WSOC

| | $C_2/\omega C_2$ | $C_2$/mGly | TDOC/WSOC |
|---|---|---|---|
| $\delta^{13}C$ | 0.49** | 0.35* | 0.41* |

** $p<0.01$; * $p<0.05$

Atmos. Chem. Phys. Discuss., doi:10.5194/acp-2016-662, 2016
Manuscript under review for journal Atmos. Chem. Phys.
Published: 22 August 2016
© Author(s) 2016. CC-BY 3.0 License.

Atmospheric Chemistry and Physics Discussions

591

Table 4. Meteorological parameters and chemical compositions (μg $m^{-3}$) of two maximum $PM_{2.5}$ between two pollution episodes in Beijing

| | T (°C) | RH (%) | V[a] (km) | $PM_{2.5}$ | OC | EC | SIA[b] | TDOC[c] |
|---|---|---|---|---|---|---|---|---|
| Event I (8/10-11/10, Before-APEC) | 16.7 ± 0.8 | 82 ± 4 | 1.5 ± 0.5 | 349 ± 57 | 45 ± 12 | 12 ± 2 | 106±39 | 2749 ± 1357 |
| Event II (18/11-21/11, After-APEC) | 4.5 ± 1.7 | 62 ± 13 | 3.5 ± 1.5 | 259 ± 102 | 60 ± 21 | 17 ± 6 | 60±32 | 831 ± 400 |

[a]V: visibility; [b]SIA: secondary inorganic ions (the sum of sulfate, nitrate and ammonium); [c]TDOC: total detected organic compounds

592

593

Atmos. Chem. Phys. Discuss., doi:10.5194/acp-2016-662, 2016
Manuscript under review for journal Atmos. Chem. Phys.
Published: 22 August 2016
© Author(s) 2016. CC-BY 3.0 License.

Atmospheric Chemistry and Physics Discussions

594

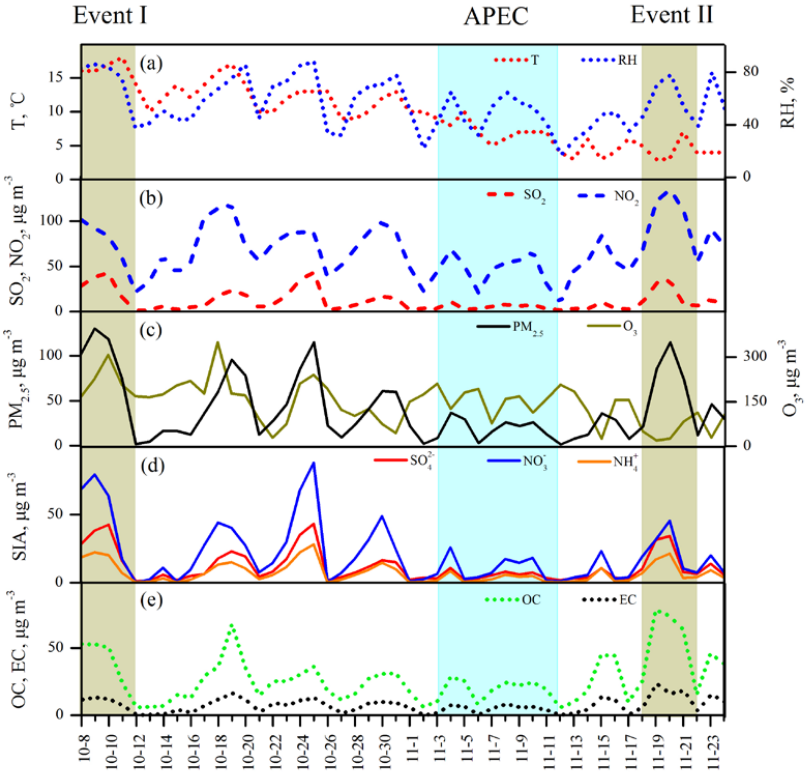


595

596 Figure 1. Temporal variations of meteorological conditions, gaseous pollutants and major components of $PM_{2.5}$
597 during the 2014 APEC campaign. (The brown shadows represent two air pollution events characterized
598 by highest $PM_{2.5}$ levels before- and after-APEC, while the blue shadow represents the APEC event).

Atmos. Chem. Phys. Discuss., doi:10.5194/acp-2016-662, 2016
Manuscript under review for journal Atmos. Chem. Phys.
Published: 22 August 2016
© Author(s) 2016. CC-BY 3.0 License.

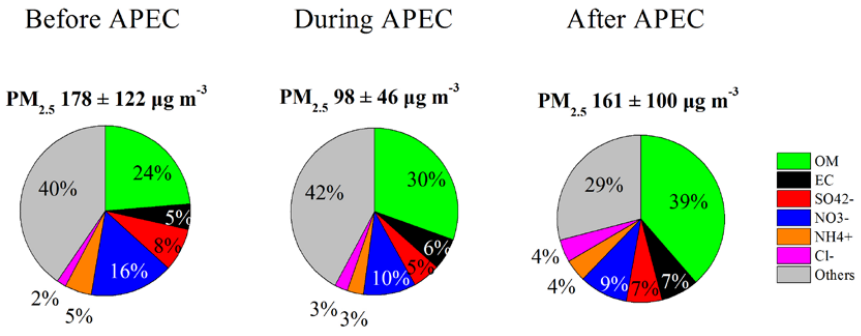


**Figure 2.** Chemical composition of $PM_{2.5}$ during the 2014 APEC campaign.

Atmos. Chem. Phys. Discuss., doi:10.5194/acp-2016-662, 2016
Manuscript under review for journal Atmos. Chem. Phys.
Published: 22 August 2016
© Author(s) 2016. CC-BY 3.0 License.

602

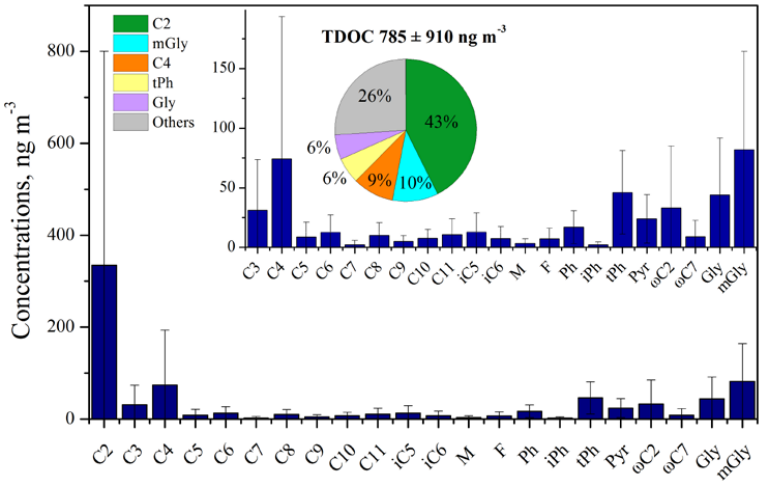


603

604 **Figure 3**. Molecular distributions of dicarboxylic acids and related compounds in $PM_{2.5}$ of Beijing, China during the
605 2014 APEC campaign. The pie chart is the average composition of total detected organic compounds
606 (TDOC) and the top number is the average mass concentration of TDOC of the whole study period.
607

Atmos. Chem. Phys. Discuss., doi:10.5194/acp-2016-662, 2016
Manuscript under review for journal Atmos. Chem. Phys.
Published: 22 August 2016
© Author(s) 2016. CC-BY 3.0 License.

608

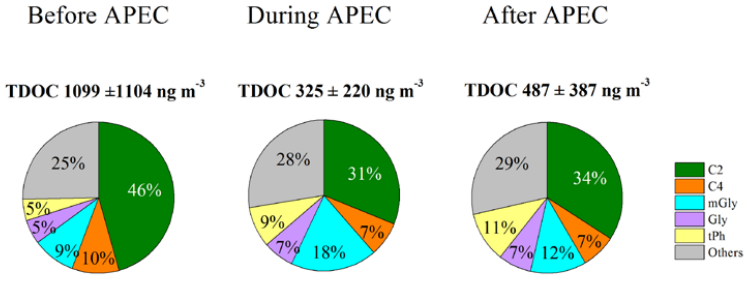


609

610 **Figure 4**. Compositions of total detected organic compounds (TDOC) in $PM_{2.5}$ during the 2014 APEC campaign.

611

Atmos. Chem. Phys. Discuss., doi:10.5194/acp-2016-662, 2016
Manuscript under review for journal Atmos. Chem. Phys.
Published: 22 August 2016
© Author(s) 2016. CC-BY 3.0 License.

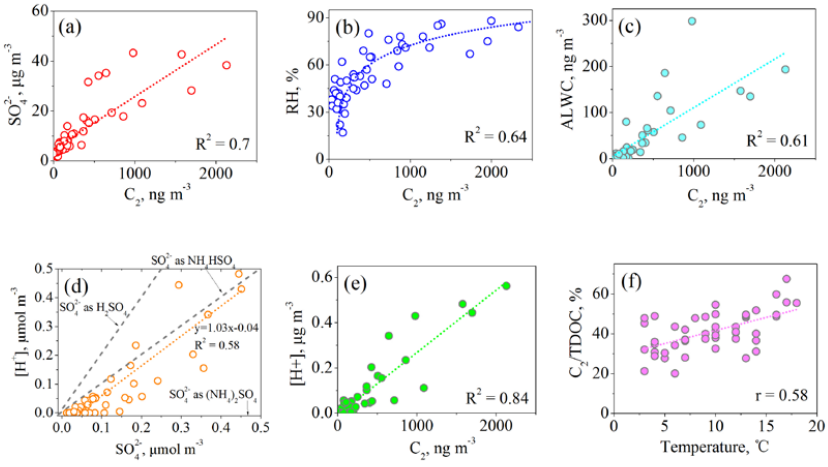


**Figure 5.** Correlation analysis for oxalic acid ($C_2$) and sulfate in $PM_{2.5}$ during the whole 2014 APEC campaign. (**a-c**) Concentrations of $C_2$ with sulfate, relative humidity (RH), and aerosol liquid water content (ALWC); (**d, e**) sulfate and $C_2$ with aerosol acidity [$H^+$] and (**f**) temperature with mass ratio of $C_2$ to total detected organic compounds ($C_2$/TDOC).

Atmos. Chem. Phys. Discuss., doi:10.5194/acp-2016-662, 2016
Manuscript under review for journal Atmos. Chem. Phys.
Published: 22 August 2016
© Author(s) 2016. CC-BY 3.0 License.

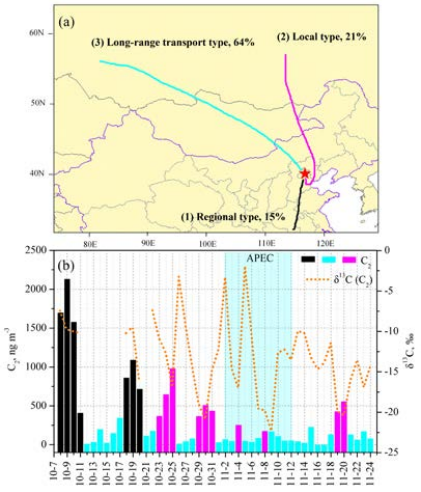


**Figure 6**. (**a**) 72-h backward trajectories determined by the National Oceanic and Atmospheric Administration Hybrid Single Particle Lagrangian Integrated Trajectory (HYSPLIT) model arriving at the sampling site to reveal the major air mass flow types during the study period. Northwesterly wind (light blue) was most frequently (64%), followed by northerly (21%, pink) and southerly (15%, black) and is defined as long-range transport, local and regional type, respectively (see the definitions in the text); (**b**) Time series of $\delta^{13}C$ values and concentration of oxalic acid during the whole study period (Colors in Fig. 6a are corresponding to those in Fig. 6b).

Atmos. Chem. Phys. Discuss., doi:10.5194/acp-2016-662, 2016
Manuscript under review for journal Atmos. Chem. Phys.
Published: 22 August 2016
© Author(s) 2016. CC-BY 3.0 License.

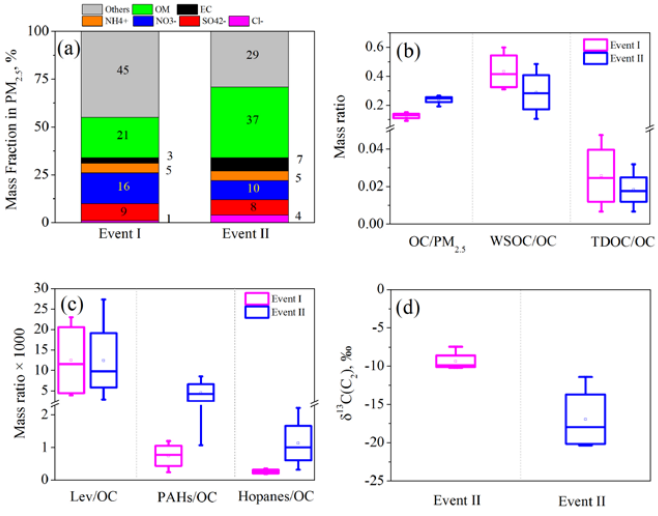


**Figure 7.** Comparison of chemical composition of $PM_{2.5}$ during two air pollution events.(**a**) Percentages of major species in $PM_{2.5}$; (**b**, **c**) mass ratios of major species and organic tracers in $PM_{2.5}$; (**d**) stable carbon isotope composition of oxalic acid ($C_2$) (Data about levoglucosan (Lev), PAHs and hopanes are cited from Wang et al (2016)).